Synthesis and Electrochemical Characterization of Graphene Nanoribbon stacks Functionalized with Buckyballs

Boštjan Genorio

University of Ljubljana, Faculty of Chemistry and Chemical Technology, Večna pot 113, 1000 Ljubljana, Slovenia

* Corresponding author: E-mail: bostjan.genorio@fkkt.uni-lj.si
Tel: +386 41 839 686

Abstract

Graphene nanoribbons were prepared from commercially-available multi-walled carbon nanotubes and *in situ* functionalized with C_{60} – buckyballs. The physical properties of the synthesized functionalized material were analyzed by scanning electron microscopy, transmission electron microscopy, evolved gas analysis and Raman spectroscopy, and were compared to non-functionalized material. Further, electrochemical characterization was done to evaluate the redox-activity and capacity of the material in Li-ion batteries. Comparison to non-functionalized material shows improved capacity at lower current densities.

Keywords Graphene nanoribbon stacks, buckyballs, C_{60}, functionalization, electrochemistry, Li-ion battery

1. Introduction

Carbon-based materials are one of the main components of energy conversion and storage devices. Various carbon allotropes can be found as catalyst supports in fuel cells, active materials in capacitors, and active components or conductive additives in batteries.[1] Recently, graphene and its sub-structure graphene nanoribbons (GNRs) – both two-dimensional allotropes of carbon – have attracted attention in the field of energy storage and conversion due to their advantageous properties such as: high conductivity, high surface area and mechanical stability. High quality – low defect graphene materials are envisioned to be a main component of future electronics, however low quality graphene materials on the other hand which still features high conductivity, high surface area, mechanical stability and facile processability are already paving their way to the commercialization. There are several reports on use of graphene in Li-ion batteries and supercapacitors,[2–4] where the addition of graphene has been shown to significantly enhance battery cycling performance and lithium storage capacity. Graphene can also effectively relieve the expansion and shrinkage of active materials during cell operation.[5] The majority of the battery literature discusses graphene as either an anode intercalation material, a volume expansion buffer, or an electron transfer medium (for both cathode and anode materials).[6] There are also reports on dual-graphite cells where graphene stacks are used as both, the anode and cathode.[7] Carbon materials are also well-known supercapacitor components for storing electrostatic charges on the electrode double-layer;[8–10]. However, the use of graphene based materials as a redox-active component of a battery system is still underexplored.

Graphene is, by itself, redox-inactive, and as a result functionalization with redox-active molecules is required. One of the redox active candidates is C_{60}-fullerene. C_{60} has a rich redox chemistry, where six electrons per molecule can be exchanged at potentials ($E_{1/2}$): –0.98, –1.37, –1.87, –2.35,–2.85, and –3.26 V vs ferrocene (Fc/Fc+).[11] Functionalization can have a major impact on the conductivity of the material; therefore an edge functionalization is preffered.[12] In order to achieve high degree of edge functionalization, high aspect ratio graphene analogues such as GNRs should be considered. Focusing on high aspect ratio GNRs, two general approaches can be applied: a) covalent functionalization, and b) non-covalent functionalization.[13] Both approaches can be used in supercapacitor and Li-ion battery electrode material synthesis. The redox-active material most commonly used in non-covalent

functionalization approach is MnO_2, which has been described in several reports.[14,15] Using a covalent functionalization approach, our group has previously shown that quinone-based functional groups on GNRs can be used as an electrode material for Li-Ion batteries.[16]

In the present study, we explored the possibility of developing an all-carbon hybrid electrode material for Li-ion battery that is conductive and redox-active at the same time. In order to develop redox activity in an all-carbon material, we focused on functionalization with buckyball-C_{60} fullerenes. All-carbon, hybrid C_{60}-GNR material was synthesized according to previously described, modified synthesis/functionalization method.[12,17] Using commercialy available multi-walled carbon nanotube (MWCNT) starting materials, this *in situ* functionalization method yielded GNRs that are edge functionalized with C_{60}. This material was characterized with scanning electron microscopy (SEM), transmission electron microscopy (TEM), evolved gas analysis (EGA), and Raman spectroscopy. Further, hybrid C_{60}-GNR material was subjected to electrochemical characterization in a Li-ion battery setup using linear scan cyclic voltammetry (CV) and galvanostatic measurements with different current rates.

2. Results and Discussion

Fullerene C_{60} is a well-known electrophile that can readily react with electron-rich systems.[18] It has also been shown that electrophiles may functionalize graphene nanoribbons by displacing alkali metal sources on graphene nanoribbons.[12.17] C_{60} functionalized GNRs (**C_{60}-GNRs**) were synthesized using a one-pot, *in situ* functionalization method with MWCNTs as starting material, Na/K alloy and C_{60} as reagents and 1,2-dimethoxyethane (DME) as solvent (Scheme 1). In the last step, methanol was used to quench all of the residual activated carbon and excess Na/K that remained after unzipping and/or C_{60} addition. To serve as a reference material, non-functionalized GNRs (**GNRs**) were also synthesized. In this case active carbon centers were quenched by methanol and no electrophile was used.

Synthesized **C_{60}-GNRs** were imaged by scanning electron microscopy (SEM) and transmission electron microscopy (TEM) (Figure 1). SEM imaging (Figure 1a) revealed high yield splitting of MWCNTs to GNRs (additional large scale SEM images can be found in Supporting Information Figure S1). Furthermore, TEM imaging shows the presence of round structures on the edges of the **C_{60}-GNRs**. These structures are <2nm in diameter, which is comparable to the van der Waals diameter of C_{60} molecules and suggests that C_{60} has been successfully covalently bound to the edge of the GNR (additional TEM images of C_{60}-GNRs can be found in Supporting Information Figure S2). However, for a clearer confirmation of covalent functionalization, more detailed high resolution TEM studies should be conducted, as similar fullerenic structures have also been shown on raw samples of combustion-generated fullerenes. [19] Regardless, according to Figure 1b the degree of possible functionalization is relatively low (for TEM images of MWCNTs and GNRs see Supporting Information Figure S3). To further explore the degree of possible functionalization, the indirect evolved gas analysis (EGA) method was used.
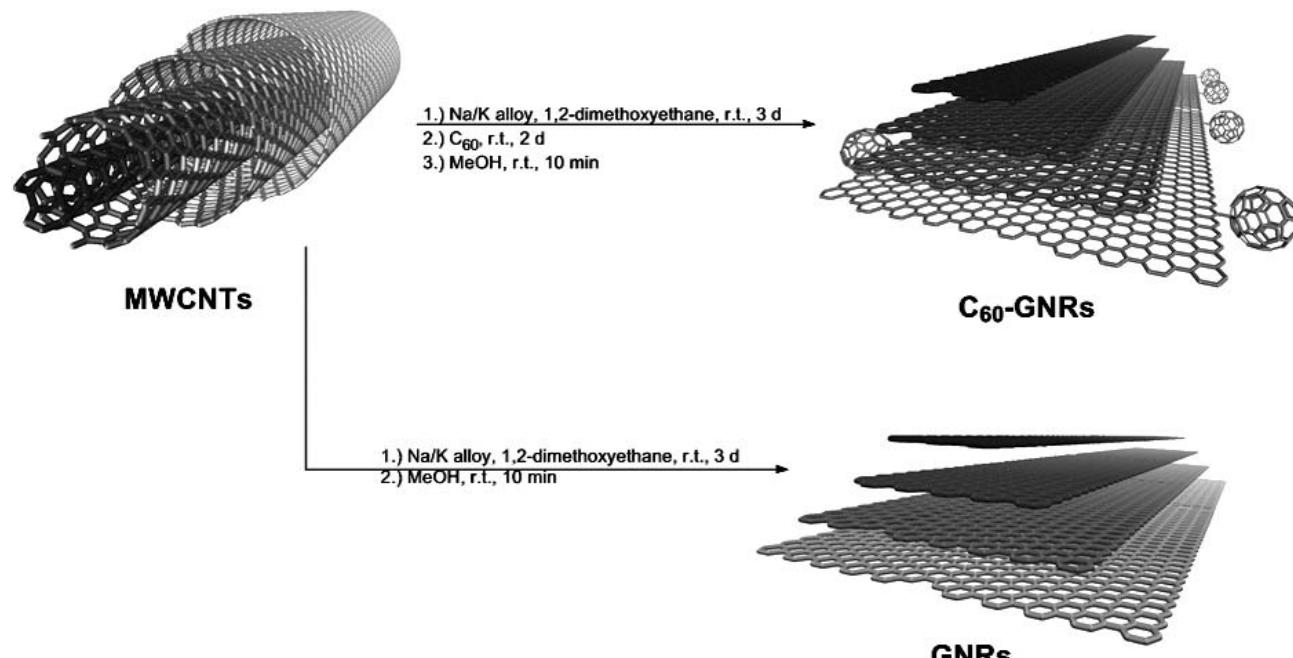
Scheme 1. Proposed reaction scheme for synthesis of C_{60}-GNRs and GNRs.

a)

b)
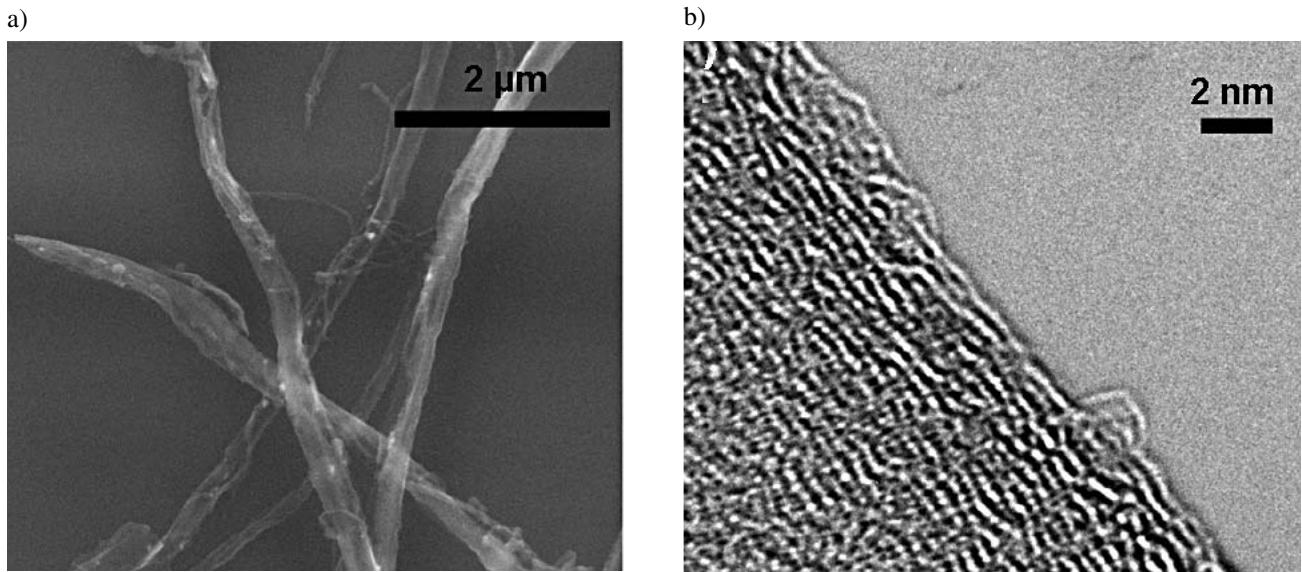
Figure 1. Images of synthesized **C$_{60}$-GNRs**. a) SEM image, b) TEM image

Comparing the EGAs of **C$_{60}$-GNRs** and **GNRs** (Figure 2) one can see that the difference in total weight loss between two samples is 13.4 % at 900 °C. MS spectra revealed that main difference in weight loss is due to adsorbed water, which is slowly released from the materials in the range between 60 °C to 260 °C and observed to be higher for **C$_{60}$-GNRs**. However, the most important difference between the functionalized and non-functionalized materials is the presence of a mass fragment at m/z = 64 (purple curve of Figure 2) in case of **C$_{60}$-GNRs**. Fragmentation of C$_{60}$ is a very complex process. It was previously shown that C$_{60}$ decomposes to several fragments with m/z M=C$_{60-2n}^{m+}$.[20] Extrapolating this formula one can assume that fragment m/z = 64 could be C$_{16}^{3+}$. Further, another publication discusses plausible mechanisms for the thermal decomposition of C^{60}.[21] They discuss possible formation of complexes with trace impurities such as oxygen, carbon, and hydrogen. Consequently, one could also expect that fragment m/z 64 could be C$_4$O$^+$ or C$_5$H$_4^+$. However, in order to confirm the chemical structure of the species with fragment m/z 64 extensive studies should be carried out, which is beyond the scope of this manuscript. However, above mentioned indicates possible presence of C$_{60}$ moieties in the composition of functionalized **C$_{60}$-GNRs**. Due to the limitations of the technique and the apparatus (the upper limit of detection is 100 AMU), one cannot directly observe the molecular mass of C$_{60}$ with m/z 720 (C$_{60}^+$) or conclude whether the functionalization is covalent or non-covalent. We have shown previously that GNRs-based materials decompose with the appearance of fragment m/z 15 (blue curve of Figure 2) in the temperature region between 400 °C and 600 °C.[12] This fragment can be found in both spectra, which indicates that both materials decompose in the same fashion. To estimate degree of functionalization, calculation based on EGA

data together with SEM images was applied (Supporting Information Table S4, Figure S5, Figure S6). Similar method was used in our previous publications.[12,22] Following experimental data were used: a) defunctionalization of **C$_{60}$-GNRs** is occurring in the temperature region between 380 °C and 600 °C, b) average size of the ribbon was 30,000 nm × 200 nm, c) weight loss related to C$_{60}$ was
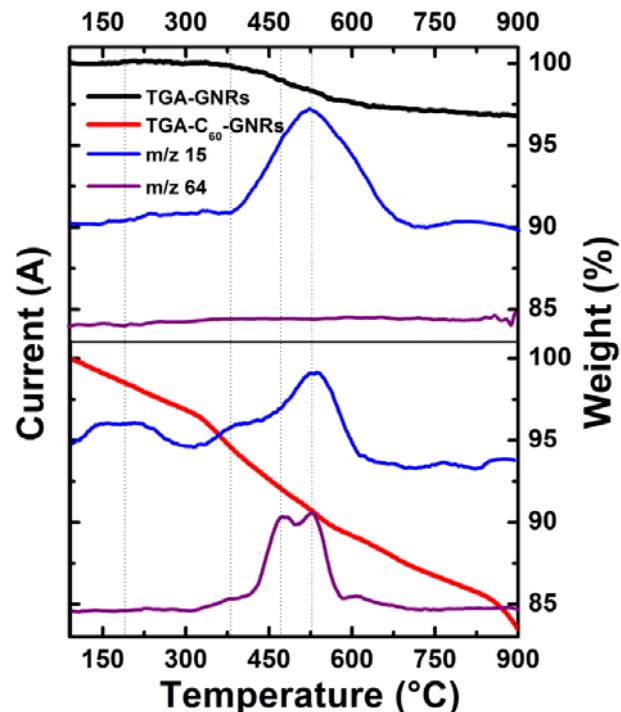

Figure 2. Evolved gas analysis. Black and red curves represent the TGA profile of **GNRs** and **C$_{60}$-GNRs** respectively. Blue and purple lines represent fragments with m/z fragments that correspond to m/z 15 and m/z 64, respectively.

3.2%. Considering above mentioned the estimated degree of functionalization is 600 atomic ppm.

Raman spectroscopy of **C$_{60}$-GNRs** was also performed to evaluate the structural quality of these materials. As shown in Figure 3, there is no noticeable difference between two spectra. They both show characteristic peaks for graphene-based materials: D at ~1352 cm^{-1}, G at ~1583 cm^{-1}, D' at ~1635 cm^{-1}, 2D at ~2708 cm^{-1}, and G+D' at ~2945 cm^{-1}.[23] The I$_D$/I$_G$ ratio was also estimated, which is an indicator of the structural disorder in graphitic materials. In both cases I$_D$/I$_G$ is relatively low – 0.6 – which indicates that the GNRs are of relatively high quality and that the functionalization process does not disrupt the quality of the supporting GNR material. We have previously shown that materials with similar I$_D$/I$_G$ ratios show relatively good electronic conductivity, which is important for energy conversion and storage devices.[12]
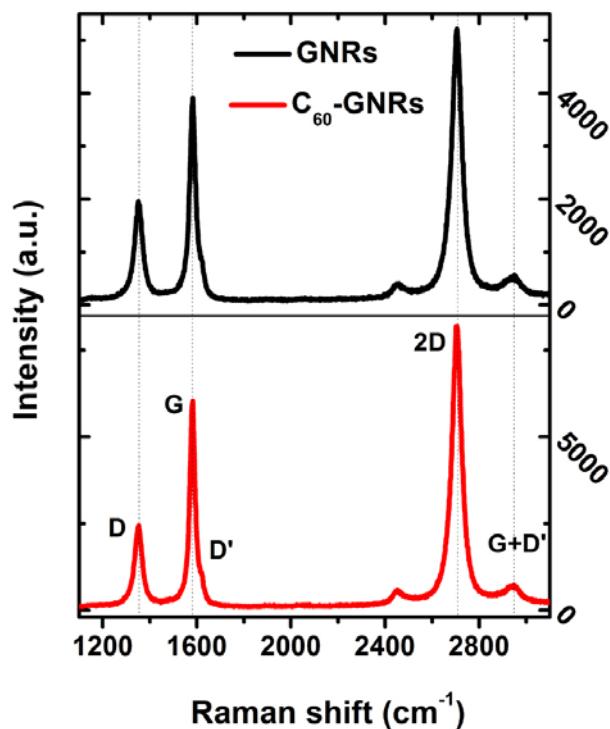

Figure 3. Raman spectra comparing non-functionalized (black curve) **GNRs** and functionalized (red curve) **C$_{60}$-GNRs**.

For electrochemical measurements, the so-called "coffee bag" battery setup with **C$_{60}$-GNRs** or **GNRs** as a working electrode and Li foil as a counter electrode was used. It is important to emphasize that working electrodes were prepared without any added binders or conductive additives, which is critical when considering practical applications for electrode materials. Cyclic voltammetry (CV) was measured for these materials (Figure 4), and from the 1st scan two oxidation peaks at 3.6 V and 3.9 V can be seen as shoulders in the red curve of Figure 4. The-

se two peaks could represent oxidation of the C$_{60}$ molecules present in the functionalized material **C$_{60}$-GNRs**. However, instead of complementary, reversible reduction peaks in the reverse scan, only one broad reduction peak starting at 2.5 V is visible. This could indicate highly irreversible redox reaction of C$_{60}$ moiety on GNRs. CV measurements also reveal that the oxidation and reduction currents slowly decrease with cycling. In contrast, non-functionalized **GNRs** show a much smaller, broad reduction peak and no oxidation peak (black curve of Figure 4). This indicates that C$_{60}$ functionalization improves the electrochemical performance of GNR materials; however, the irreversibility of electrochemistry is a definite drawback for possible application in real Li-ion battery systems. Similar electrochemistry was also observed previously for the pure C$_{60}$ which was used as a cathode in Li-ion battery setup.[24] The electrochemical irreversibility of **C$_{60}$-GNRs** material could also be the result of a reaction between oxidized species and the electrolyte or due to formation of a solid-electrolyte interphase on the electrode. Nevertheless, the functionalization showed improved electrochemistry when compared to non-functionalized material.
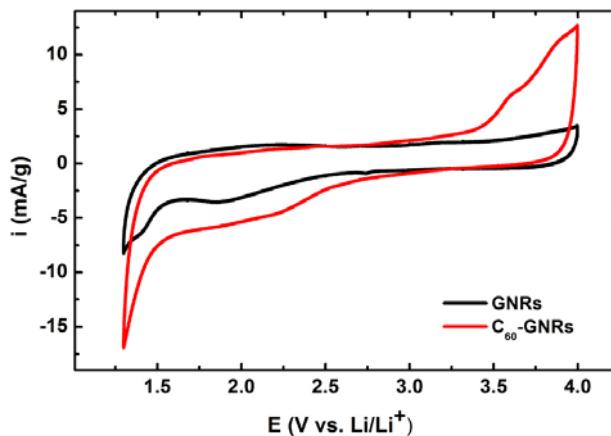

Figure 4. Cyclovoltammograms for non-functionalized **GNRs** (black curve) and functionalized **C$_{60}$-GNRs** (red curve); scan rate 0.1 mV/s.

Charge–discharge rate capability is one of the most important properties of cathode materials that can be used in lithium batteries. Galvanostatic rate capability tests for both of the materials: **C$_{60}$-GNRs** and **GNRs** were performed (Figure 5), which show higher capacities for the functionalized **C$_{60}$-GNRs** material. At low current densities the capacity for **C$_{60}$-GNRs** (22 mAh/g) is twice that of the non-functionalized **GNRs** (12 mAh/g) (for charge-discharge curves see Supporting Information Figures S7 and S8). However, at higher current densities (800 mA/g) the capacity difference between two materials decreases until the capacities are equal (6 mAh/g). This means that rate performance for **C$_{60}$-GNRs** is actually worse than for **GNRs**.

As functionalization does not noticeably increase the surface area, one can expect that the difference in capacity for low current densities is related to activity of the functional groups. Furthermore, it is possible that the slow redox kinetics of C_{60} or lower the conductivity of the functionalized material relative to non-functionalized, leading to the poor rate capability. It is known from previous reports that conductivity can decrease with functionalization.[1] Different contact resistance between single **C60-GNRs** can also impact fast capacity drop at higher current densities. We have shown previously, that alignment of the graphene nanoribbons drastically affect the contact resistance.[17] In this respect, spherical C_{60} functionalities might disturb favorable alignment, increase contact resistance, and consequently cause fast capacity drop at higher current densities. However, the reason for the poor rate capability of these materials remains unclear at this point.
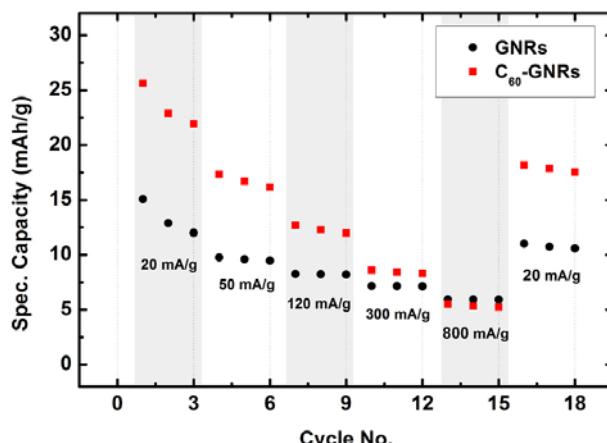

Figure 5. Rate capability for non-functionalized **GNRs** (black circles) and functionalized **C$_{60}$-GNRs** (red squares) at 20 mA/g, 50 mA/g, 120 mA/g, 300 mA/g, and 800 mA/g current densities.

3. Conclusions

Functionalization of GNRs with electroactive moieties is an approach that could lead to novel cathode materials for a variety of battery applications. In the present study, MWCNTs were split to GNRs *in situ* and functionalized with C_{60} fullerenes. These functionalized **C$_{60}$-GNR** materials were compared to non-functionalized **GNRs** and characterized using a variety of imaging and electrochemical techniques. SEM imaging revealed high yield splitting of MWCNTs to GNRs and TEM imaging shows the presence of spherical structures on the GNR edges that suggest the presence of attached C_{60}. Further, EGA analysis supports the hypothesis of successful functionalization of these structures with C_{60}. In particular, it reveals that the mass fragment at m/z = 64 is present only for the functionalized **C$_{60}$-GNRs** material. As the fragment at m/z = 64 is also one of the fragments observed for pure C_{60}, it could be an indicator of the presence of C_{60}

functional groups. These results favor the hypothesis of successful functionalization, however, at this time it cannot be confirmed conclusively whether C_{60} molecules are adsorbed or covalently bound. The graphitic nature of the functionalized material was confirmed by Raman spectroscopy, where bands typical for graphene are present. Further, a relatively small I_D/I_G ratio is a good indicator of low concentration of structural defects in the graphene lattice, and confirms that the functionalization with C_{60} does not disrupt the quality of the GNR supporting material. Electrochemical experiments, in particular CV, showed irreversible redox reaction of functionalized material in first cycles. Galvanostatic cycling was performed under various current densities for both samples – **C$_{60}$-GNRs** and **GNRs** and compared. Results showed doubled capacity for **C$_{60}$-GNRs** on one hand, but worse rate performance on the other hand. Nevertheless, the improved capacity at low current densities for functionalized GNR materials, in combination with the simple assembly method of the electrode where no binders or conductive additives are used, make these materials attractive for further investigation. These materials may also be attractive for beyond lithium systems, e.g. Mg-ion batteries, where reversible cycling of Mg with pure C_{60} was shown recently.[25]

4. Experimental

4. 1. Materials

All reactions were performed in dried glassware under an Ar atmosphere unless stated otherwise. Reagent grade 1,2-dimethoxyethane was degassed with Ar, refluxed over Na/K alloy in an Ar atmosphere and freshly distilled. Other solvents were used without further distillation. NTL – M grade MWCNTs were donated by Nanotech Labs, Inc. (5T10M10). All other commercially available reagents were used as received. Liquid Na/K alloy was prepared in a vial inside of a N_2 glove box by pressing together freshly cut K (1 molar equivalent) and Na (0.22 molar equivalents) chunks using tweezers to facilitate the melting process. Amounts of liquid Na/K alloy indicated are by volume. *Caution: All synthetic steps involving Na/K alloy should be carried out with extreme caution under strict exclusion of air or moisture, under inert gas and appropriate personal protection (hood, blast shields, face shield, protective and fire resistant clothing) should be used and worn at all times.* C_{60} was obtained from Sigma-Aldrich and used as received without further purification. Milli-Q water was used during purification of the products.

4. 2. Synthesis of C$_{60}$ Functionalized Graphene Nanoribbons Stacks (C$_{60}$-GNRs)

To an vacuum oven-dried (200 °C) 250 mL round-bottom flask containing a magnetic stir bar were added the MWCNTs (100 mg, 8.3 mmol). The vessel was then

transferred to a Ar glove box where freshly distilled 1,2-dimethoxyethane (43 mL) and liquid Na/K alloy (0.1 mL) were added. The flask containing the suspension was then sealed with a septum and was vigorously stirred (450 RPM) at room temperature in glove-box for 3 d. The reaction suspension was then quenched by the addition of the C_{60} (180 mg, 0.25 mmol) and left to stir at the room temperature for an additional day. Reaction mixture was then transferred out of the glove-box where methanol (20 mL, 500 mmol) was added to quench any excess Na/K alloy and the mixture was stirred at room temperature for 10 min. For workup, the reaction mixture was filtered over a 0.2 μm pore size PTFE membrane. The filter cake was successively washed with THF (100 mL) and CS_2 (100 mL) and exposed to Soxhlet extraction for 8 h to remove the unreacted C_{60}. After extraction solid was dispersed in CS_2 (50 mL) and sonicated for 1 h. Solution was then filtrated again using PTFE 0,2 μm filter pad. The filter cake was successively washed with THF (100 mL), *i*-PrOH (100 mL), H_2O (100 mL), *i*-PrOH (50 mL), THF (50 mL), Et_2O (50 mL) and dried under high vacuum. Mass of the dried product was 80.6 mg.

4. 3. Synthesis of Non-functionalized Graphene Nanoribbons Stacks (GNRs)

The same procedure as described above for synthesis of **C_{60}-GNRs** was followed, except that step where C_{60} was added was omitted.

4. 4. Electron Microscopy

Samples were dispersed in chlorobenzene and bath sonicated using an ultrasonic cleaner for 15 min for a quick dispersion. A drop was cast on a 100 nm SiO_2/Si substrate and large area low resolution images were taken at 20 kV under FEI Quanta 400 ESEM FEG scanning electron microscope. For more refined images of the synthesized structure at higher resolution, a JEOL 2010 transmission electron microscope was used with the sample drop cast on a coated TEM grid.

4. 5. Evolved Gas Analysis (EGA)

Thermogravimetric measurements were performed on a Netzsch 449 F3 Jupiter® instrument under a dynamic Ar (5.0) flow with a flow rate of 60 mL/min in a temperature range from 25 °C to 900 °C. A heating rate of 10 K/min was used. About 5 mg of sample was placed in alumina (Al_2O_3) crucible. Simultaneously mass spectrometry was performed on MS 403C Aëolos® with detector SEM Chenneltron and system pressure of 2×10^{-5} mbar. Gasses evolved under TG heat treatment were transferred to mass spectrometer through transfer capillary: quartz ID 75 μm which was heated up to 220 °C. The upper limit of the mass spectrometer detector was 100 AMU.

4. 6. Raman Spectroscopy

The Raman spectra were acquired using a Renishaw Raman RE01 microscope with 40 × lens; 514 nm wavelength LASER was used for excitation.

4. 7. Electrochemical Tests

C_{60}-GNRs and **GNRs** (~5 mg) were suspended in THF (15 mL) in an ultrasonic bath for 10 min until the suspension was homogeneous. The suspension was then filtered through a glassy fiber Whatman GF/A (battery separator) in a Millipore membrane filtration system. The diameter of the filtration disc was 25 mm. The filtration resulted in a uniformly distributed material on a glassy fiber separator, from which 12mm diameter discs were cut out. These discs were then transferred to an Ar glove-box and allowed to dry for 1 day. Modified Swagelok battery cells were assembled in the glove box (water and oxygen levels <1 ppm). For every cell, 5 drops of 1M $LiPF_6$ in ethylene carbonate/diethyl carbonate (EC/DEC)=1:1 (vol.), purchased from Merck (LP40), were used. A lithium foil (Aldrich, 0.75mm thick) as counter electrode was rolled and cut prior to assembly.

Electrochemical measurements were performed on a VMP3 potentiostat/galvanostat (Bio-Logic, France). Batteries were cycled be– tween 4.0 and 1.3 V versus metallic Li. CV measurements were performed in a two-electrode cell with a scan rate of 0.1 mV/s. Galvanostatic cycling (rate capability) was performed at various current densities in a wide range from 20 to 800 mA/g.

5. Acknowledgements

6. References

1. Rao, C.; Sood, A. *Graphene: Synthesis, Properties, and Phenomena*; Rao, C. N. R.; Sood, A. K., Eds.; 1st ed.; Wiley-VCH Verlag GmbH & Co. KGaA: Weinheim, 2013.
2. Luo, B.; Liu, S.; Zhi, L. *Small* **2012**, *8*, 630–646. http://dx.doi.org/10.1002/smll.201101396
3. Zhang, L. L.; Zhou, R.; Zhao, X. S. *J. Mater. Chem.* **2010**, *20*, 5983–5992. http://dx.doi.org/10.1039/c000417k
4. Huang, Y.; Liang, J.; Chen, Y. *Small* **2012**, *8*, 1805–1834. http://dx.doi.org/10.1002/smll.201102635

5. Liang, M.; Zhi, L. *J. Mater. Chem.* **2009**, *19*, 5871–5878. http://dx.doi.org/10.1039/b901551e

6. Raccichini, R.; Varzi, A.; Passerini, S.; Scrosati, B. *Nat. Mater.* **2014**, *14*, 271–279. http://dx.doi.org/10.1038/nmat4170

7. Placke, T.; Fromm, O.; Lux, S. F.; Bieker, P.; Rothermel, S.; Meyer, H.-W.; Passerini, S.; Winter, M. *J. Electrochem. Soc.* **2012**, *159*, A1755–A1765. http://dx.doi.org/10.1149/2.011211jes

8. Zhu, Y.; Li, L.; Zhang, C.; Casillas, G.; Sun, Z.; Yan, Z.; Ruan, G.; Peng, Z.; Raji, A.-R. O.; Kittrell, C.; Hauge, R. H.; Tour, J. M. *Nat. Commun.* **2012**, *3*, 1225. http://dx.doi.org/10.1038/ncomms2234

9. Kotal, M.; Bhowmick, A. K. *J. Phys. Chem. C* **2013**, *117*, 25865–25875. http://dx.doi.org/10.1021/jp4097265

10. Zhang, C.; Peng, Z.; Lin, J.; Zhu, Y.; Ruan, G.; Hwang, C.-C.; Lu, W.; Hauge, R. H.; Tour, J. M. *ACS Nano* **2013**, *7*, 5151–5159. http://dx.doi.org/10.1021/nn400750n

11. Echegoyen, L.; Echegoyen, L. E. *Acc. Chem. Res.* **1998**, *31*, 593–601. http://dx.doi.org/10.1021/ar970138v

12. Genorio, B.; Lu, W.; Dimiev, A. M.; Zhu, Y.; Raji, A.-R. O.; Novosel, B.; Alemany, L. B.; Tour, J. M. *ACS Nano* **2012**, *6*, 4231–4240. http://dx.doi.org/10.1021/nn300757t

13. Genorio, B.; Znidarsic, A. *J. Phys. D. Appl. Phys.* **2014**, *47*, 094012. http://dx.doi.org/10.1088/0022-3727/47/9/094012

14. Li, L.; Raji, A. R. O.; Tour, J. M. *Adv. Mater.* **2013**, *25*, 6298–6302. http://dx.doi.org/10.1002/adma.201302915

15. Liu, M.; Tjiu, W. W.; Pan, J.; Zhang, C.; Gao, W.; Liu, T. *Nanoscale* **2014**, *6*, 4233–4242. http://dx.doi.org/10.1039/c3nr06650a

16. Pirnat, K.; Bitenc, J.; Jerman, I.; Dominko, R.; Genorio, B. *ChemElectroChem* **2014**, *1*, 2131–2137. http://dx.doi.org/10.1002/celc.201402234

17. Genorio, B.; Peng, Z.; Lu, W.; Hoelscher, B. K. P.; Novosel, B. J.; Tour, J. M. *ACS Nano* **2012**, *6*, 10396–10404. http://dx.doi.org/10.1021/nn304509c

18. Wudl, F. *Acc. Chem. Res.* **1992**, *25*, 157–161. http://dx.doi.org/10.1021/ar00015a009

19. Goel, A.; Howard, J. B.; Sande, J. B. V. *Carbon N. Y.* **2004**, *42*, 1907–1915. http://dx.doi.org/10.1016/j.carbon.2004.03.022

20. Baba, M. S.; Narasimhan, T. S. L.; Balasubramanian, R.; Mathews, C. K. *J. Phys. Chem.* **1995**, *99*, 3020–3032. http://dx.doi.org/10.1021/j100010a010

21. Sundar, C. S.; Bharathi, A.; Hariharan, Y.; Janaki, J.; Sankara Sastry, V.; Radhakrishnan, T. S. *Solid State Commun.* **1992**, *84*, 823–826. http://dx.doi.org/10.1016/0038-1098(92)90098-T

22. Lu, W.; Ruan, G.; Genorio, B.; Zhu, Y.; Novosel, B.; Peng, Z.; Tour, J. M. *ACS Nano* **2013**, *7*, 2669–2675. http://dx.doi.org/10.1021/nn400054t

23. Dresselhaus, M. S.; Jorio, a.; Saito, R. *Annu. Rev. Condens. Matter Phys.* **2010**, *1*, 89–108. http://dx.doi.org/10.1146/annurev-conmatphys-070909-103919

24. Seger, L.; Wen, L.-Q.; Schlenoff, J. B. *J. Electrochem. Soc.* **1991**, *138*, 81–82. http://dx.doi.org/10.1149/1.2085516

25. Zhang, R.; Mizuno, F.; Ling, C. *Chem. Commun.* **2014**, *51*, 1108–1111. http://dx.doi.org/10.1039/C4CC08139K

Povzetek

Opisana je sinteza s fulereni-C_{60} funkcionaliziranih grafenski nanotrakov, ki so bili pripravljeni iz komercialno dostopnih večstenskih ogljikovih nanocevk po *in situ* postopku. Fizikalne lastnosti sintetiziranega materiala so bile analizirane z elektronsko vrstično mikroskopijo, presevno elektronsko mikroskopijo, analizo sproščenega plina in ramansko spektroskopijo. Lastnosti funkcionaliziranega materiala so bile nato primerjane z nefunkcionaliziranim. Oba materiala, tako funkcionaliziran, kot nefunkcionaliziran sta bila nato ovrednotena tudi elektrokemijsko. Določena je bila redoks ativnost in kapaciteta obeh v litij-ionskih baterijah. Primerjava obeh materialov je pokazala izboljšano kapaciteto funkcionaliziranega materiala pri nizkih tokovnih gostotah.

Synthesis and Electrochemical Characterization of Graphene Nanoribbon stacks

Functionalized with Buckyballs – Supporting Information

Bostjan Genorio

University of Ljubljana, Faculty of Chemistry and Chemical Technology, Večna pot 113, 1000

Ljubljana, Slovenia

Corresponding author: E-mail: bostjan.genorio@fkkt.uni-lj.si

Tel: +386 41 839 686

Table of Contents

Figure S1. Large scale SEM images of: a) M-grade NTL MWCNTs, b) GNRs and c) C_{60}-GNRs
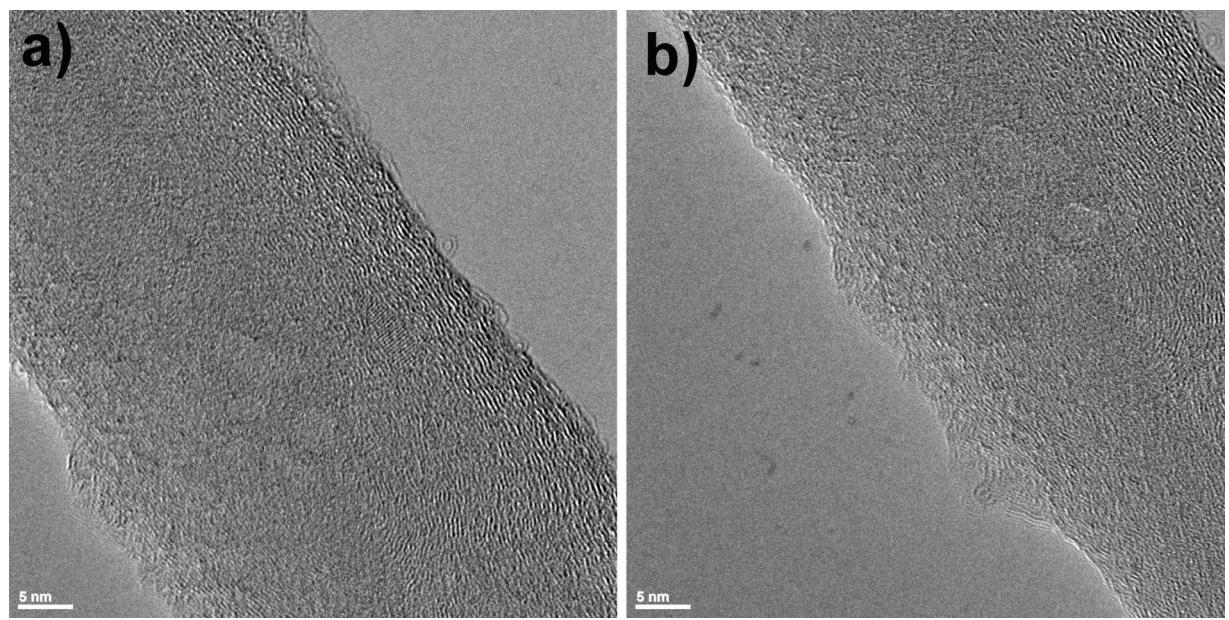
Figure S2. TEM images of C_{60}-GNRs.
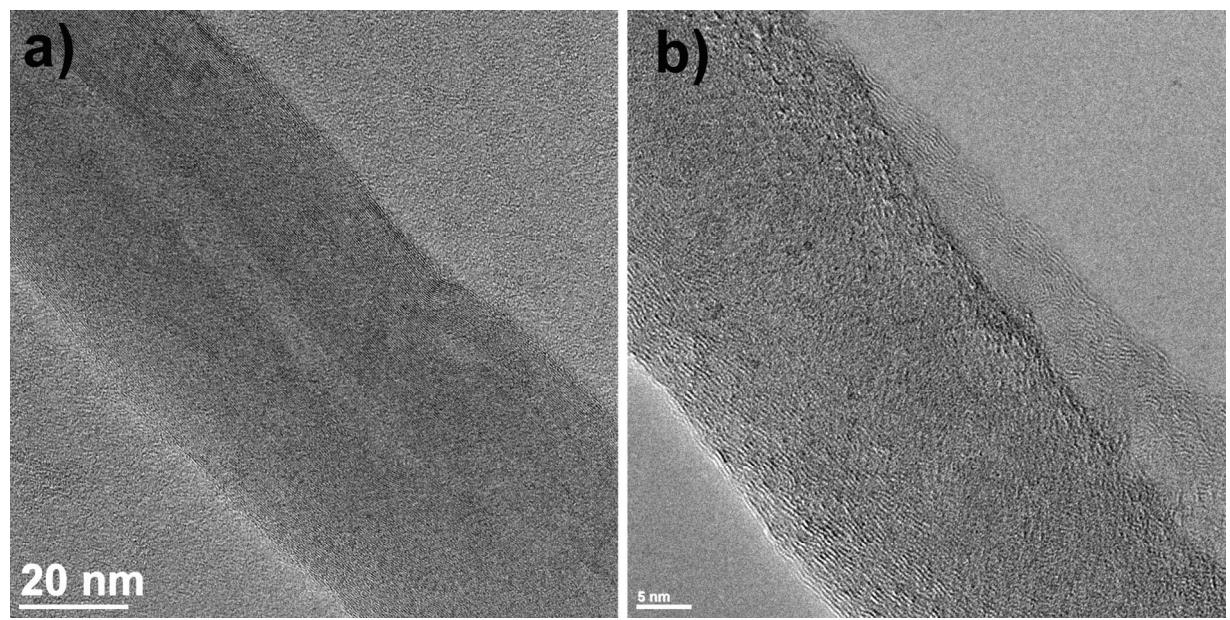
**Figure S3**. TEM images of a) M-grade NTL MWCNTs and b) GNRs

F = Functional Group
C = Carbon
$n_{C(edges)} = n_{F(edges)}$
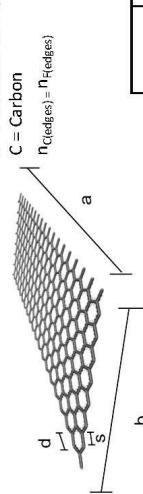
	value	unit
a	30000	nm
b	200	nm
d	0.267	nm
s	0.154	nm
$M_{(C)}$	12	g/mol
$M_{(F)}$	720	g/mol
Weight loss % obtained by subtracting GNRs-TG from C60-GNRs TG (region between 380 °C and 600 °C)	3.20	%

color	origin of data
(blue)	experiment
(olive)	literature
(red)	calculated

	value	unit
$N_{C(all)}$	194,561,992	#atoms
$n_{C(all)}$	3.23E-16	mol
$m_{C(all)}$	3.88E-15	g

	value	unit
$N_{C(edges)}$	226,451	#atoms
$n_{C(edges)}$	3.76E-19	mol
$m_{C(edges)}$	4.51E-18	g

$m_{(ribbon)}$	3.88E-15	g
$m_{(\Sigma F)}$	2.71E-16	g
Wt	6.53	%

atomic % of the edges	0.12

	value	unit
$n_{F(TGA)}$	0.004444444	mol
$n_{C(all\ TGA)}$	8.066666667	g

Ratio of n_C (all TGA) : $n_{F(TGA)}$	1815 :1

Ratio of n_C (all) : $n_{C(edges)}$	859 :1

Degree of functionalization (N_C (funct.)/$N_{C(all)}$ *100)	0.06	atomic %

check 0.057057813

Ratio of functionalized edges on GNRs	value	unit
	47	%

Table S4. Calculation of degree of functionalization.
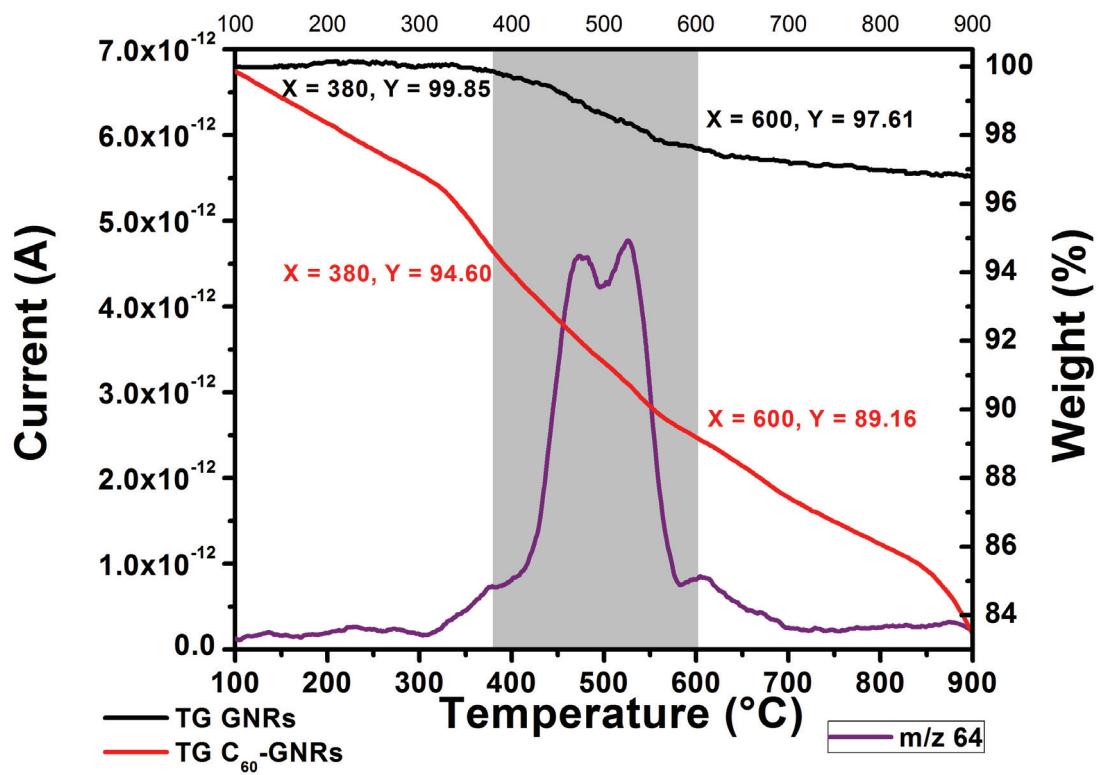
Figure S5. Evolved gas analysis.
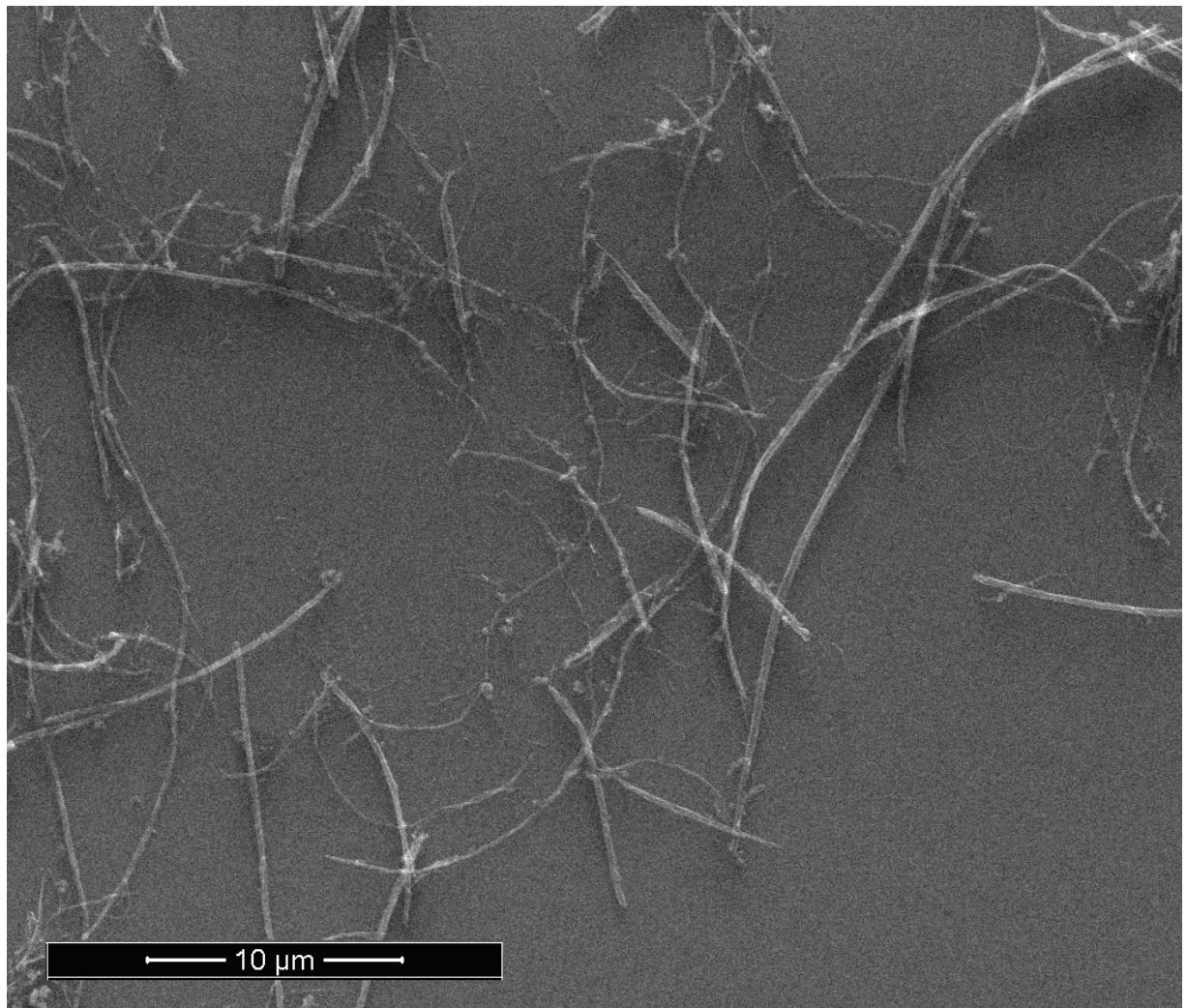
Figure S6. Large scale C_{60}-GNRs SEM image.

a) Galvanostatic curves for GNRs
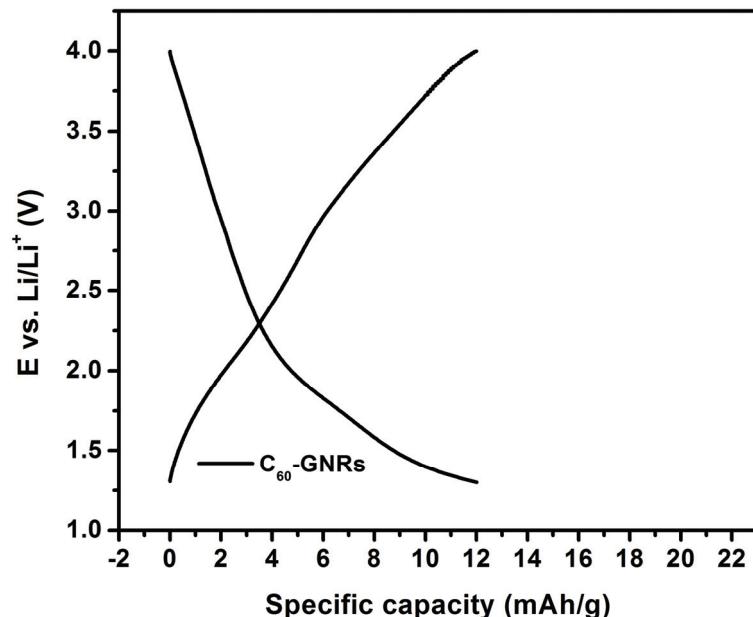
b) Galvanostatic curves for C60-GNRs
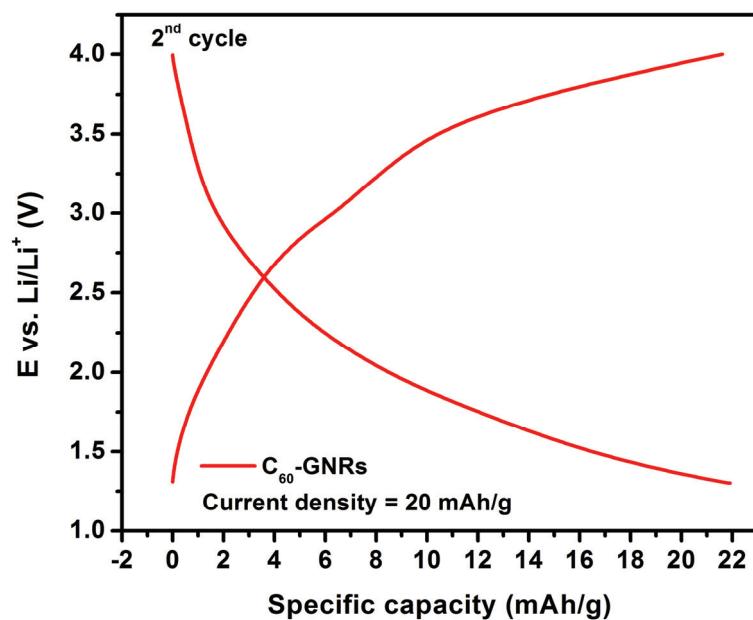
Figure S7. Galvanostatic curves for: a) GNRs and b) C_{60}-GNRs.

a)

GNRs Charge-Discharge Curves at Diffrent Current Densities

300mAh/g
120mAh/g
50mAh/g 800mAh/g 20mAh/g

20mAh/g

E vs. Li/Li$^+$ (V)

Time (s) — GNRs

b)

C$_{60}$-GNRs Charge-Discharge Curves at Diffrent Current Densities

300mAh/g
120mAh/g
50mAh/g 800mAh/g

20mAh/g
20mAh/g

E vs. Li/Li$^+$ (V)
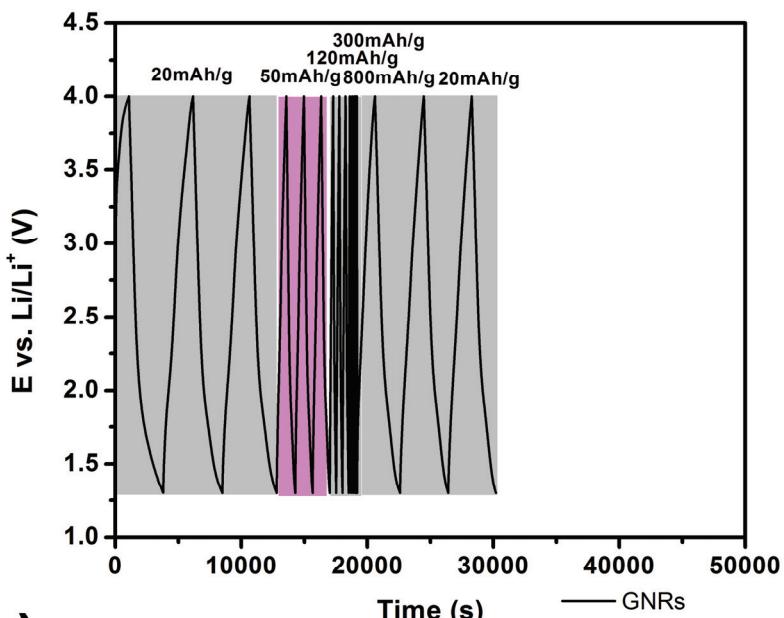
Time (s) — C$_{60}$-GNRs
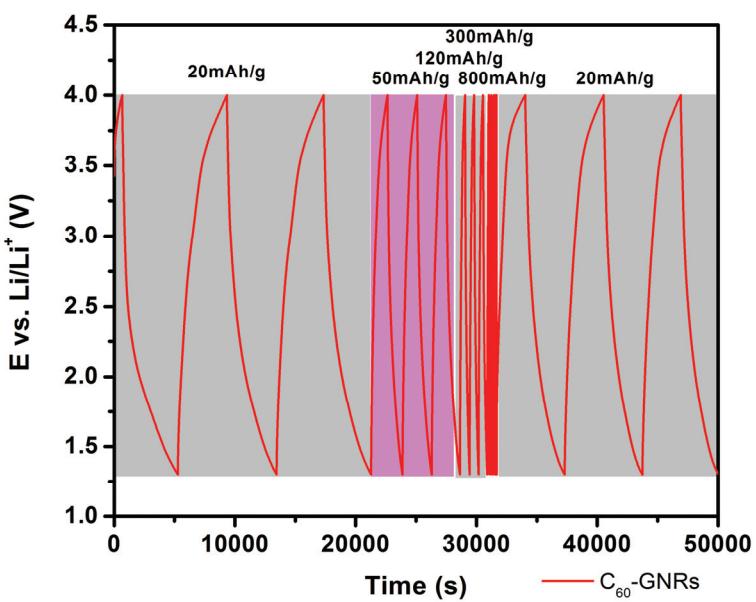
Figure S8. Charge-Discharge curves at different current densities: a) GNRs and b) C$_{60}$-GNRs